Why should axon diameter mapping use low frequency OGSE? Insight from simulation

Ivana Drobnjak[1], Hui Zhang[1], Andrada Ianus[1], Enrico Kaden[1], and Daniel C Alexander[1]
[1]*Centre for Medical Image Computing, Department of Computer Science, University College London, London, London, United Kingdom*

TARGET AUDIENCE: Researchers studying brain microstructure, especially axon diameter.

PURPOSE: This work aims to identify the optimal sequence that maximizes sensitivity to axon diameter in practical applications. Axon diameter statistics provide information about the function and performance of white matter pathways. Hence imaging axon diameter could provide insight into basic brain operation as well as neuronal diseases that alter axon diameter distribution. Whilst the majority of current diffusion imaging methods use Pulsed Gradient Spin-Echo (PGSE) sequence, various authors suggest that Oscillating Gradient Spin-Echo (OGSE) offers benefits over PGSE for imaging pore sizes [1-6]. Although short diffusion time has been speculated as a possible explanation, this has yet to be systematically investigated. Here we address this question for axon diameter mapping by looking at all possible combinations of OGSE and PGSE sequences. We consider parallel axons with known orientation as well as more realistic cases of unknown orientation and fibre dispersion typical in brain white matter. This is, to our knowledge, the first time signal sensitivity to axon diameter has been studied using diffusion signal analysis, and the first time fibre dispersion is taken into account.

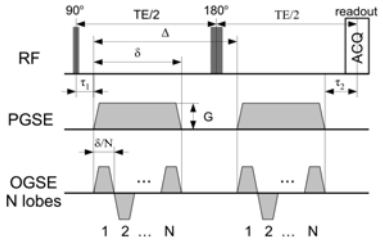

Figure 1: Illustration of PGSE and OGSE sequences used here.

METHODS: Simulations on a simple two-compartment white matter model (with non-permeable infinite cylinders) are used to investigate a wide space Λ of clinically plausible PGSE and OGSE sequence parameters with trapezoidal diffusion gradient waveforms [11] (Figure 1). N is the number of lobes and when N=1, OGSE reduces to PGSE. Two tissue models are used: 1) parallel fibres of orientation **n** [7,8] and 2) fibres dispersed about the dominant orientation with a scalar parameter $\boldsymbol{\kappa}$ following a Watson distribution [9]. The signal model is $S^*=S_0(f\ S_r+(1-f)S_h)$ where $S_0=\exp(-TE(\delta,\Delta)/T_2)$ is normalized by proton density; f intracellular volume fraction; S_h the extracellular signal using the diffusion tensor and tortuosity model $D_\perp=D_\parallel(1-f)$; S_r is the intracellular signal with intrinsic diffusivity equal to $D_\parallel$. Signal sensitivity to axon diameter a is measured by the derivative of the signal with respect to a, $S^{*\prime}(a)=S_0\ f\ S_r'(a)$. We set f=0.7, $D_\parallel=1.7\times10^{-9}m^2s^{-1}$, $a\in[0,10]\mu m$, $\boldsymbol{\kappa}\in\{8,16,32\}$ and T_2=70ms to match standard values in the white matter at 3T. Λ is defined as $G\in[0,300]$mT/m, $\delta\in[0,60]$ms, $\Delta\in[\delta+P180,100]$ms, $N\in[1,10]$, P180=10ms. Note that b-values and TE are not fixed and the sequence parameters can take any values in Λ. The simulations are done using the open source software MISST [2,10], available at "http://www.nitrc.org/projects/misst", and take a few minutes to compute on a standard computer.

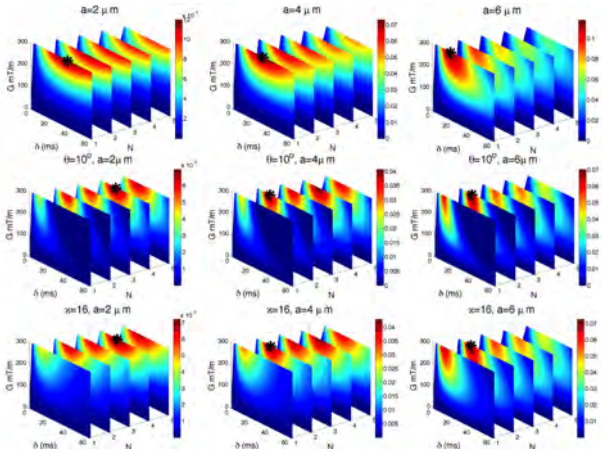

Figure 2: Impact of G, δ, and N on sensitivity $S^{*\prime}(a)$ for θ=0° i.e. **n⊥G** (top), θ=10° (middle), dispersion κ=16 (bottom) for $a\in\{2,4,6\}\mu m$ from left to right. The absolute value of $S^{*\prime}(a)$ is color coded with dark red being the highest value. Maximum intensity points are marked with a black star. $S^{*\prime}(a)$ is in 1/μm.

RESULTS: Figure 2 shows sensitivity $S^{*\prime}(a)$ in space Λ for a range of axon diameters with $\Delta=\delta+P180$ which we show is a good approximation for the optimal Δ (data not shown). The top row shows that for **n⊥G** ($\theta=\angle(\mathbf{n},\mathbf{G})=0°$) N=1 always gives maximum sensitivity. When θ>0°, N>1 provides higher sensitivity. The middle row shows N=4 or N=2 to be optimal for θ=10° which corresponds to HARDI acquisition of 30 directions. Similar results are obtained for fibre dispersion and the bottom row shows results for **κ=16** typical of corpus callosum. Figure 3 shows that the sensitivity differences in Figure 2 are significant enough to make a difference in identifiable diameters in the presence of noise. The top row shows the actual signal $S^*(a)$. The middle and bottom rows show the signal difference, which, owing to non-linearity of $S^*(a)$, is calculated as $|S^*(a)-S^*(a-1)|$ (middle) and $|S^*(a)-S^*(a-0.5)|$ (bottom) investigating diameter resolutions of 1 and 0.5μm respectively. Curve areas above the standard deviation (1/SNR) lines are larger than the noise and hence considered identifiable. Table 1 shows the smallest identifiable axon diameter, from Figure 3, for a range of G and SNRs.

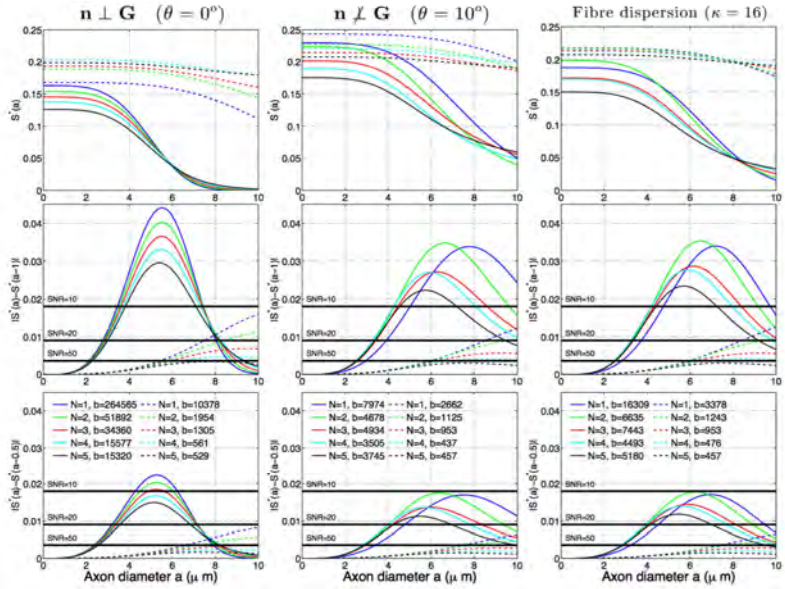

Figure 3 Signal $S^*(a)$ (top), signal difference for diameter difference of 1μm (middle) and 0.5μm (bottom) for G=300mT/m (full lines), and G=60mT/m (dashed lines). Each line is generated with optimal sequence combination from Figure 2. b value is in s/mm^2.

DISCUSSION: This study shows that although PGSE always gives maximum sensitivity for the simple case of gradients perfectly perpendicular to straight parallel fibres, low frequency OGSE provides higher sensitivity in real-world scenarios where fibres have unknown or dispersed orientation. This is a novel and fundamental insight into both sequences and their benefits for imaging axon diameter. Our finding does not support the traditional view that short effective diffusion time increases sensitivity to small axons, e.g. for **n⊥G**, T_2 large or TE fixed, the best choice of δ is as long as possible (data not shown) and N as low as possible. Combined sensitivity to axon diameter and diffusivity for **n⊥G** on the other hand can benefit from higher frequencies [2-5]. Our results show that on current clinical scanners (G=60mT/m, SNR=20) axons below 6μm are indistinguishable from zero. Stronger gradient systems such as the MGH Connectom G=300mT/m can extend this sensitivity limit down to 2-3μm, and for these, the benefits from OGSE are even greater. Here we assume independence of the axon diameter and T_2, and set $D_\parallel$, f and P180 to commonly used values. Typical variations in these assumptions do not significantly change our results (up to a couple of ms in the optimal δ), and hence do not affect our conclusions. Areas of future work will involve collections of cylinders of varying diameters and more complex extracellular space models.

		N=1			N>1		
	SNR / G	10	20	50	10	20	50
1) **n** ⊥ **G**	60mT/m	7.2	6.0	4.6	7.5 (N=2)	6.1 (N=2)	4.7 (N=2)
	80 mT/m	6.2	5.1	4.0	6.4 (N=2)	5.2 (N=2)	4.1 (N=2)
	150 mT/m	4.5	3.7	3.0	4.5 (N=2)	3.8 (N=2)	3.0 (N=2)
	300 mT/m	3.2	2.7	2.1	3.2 (N=2)	2.7 (N=2)	2.1 (N=2)
2) **n** ∦ **G** $\theta=10°$	60 mT/m	7.8	6.5	5.0	7.7 (N=2)	6.3 (N=2)	4.9 (N=2)
	80 mT/m	6.9	5.7	4.5	6.7 (N=2)	5.4 (N=2)	4.2 (N=2)
	150 mT/m	5.3	4.4	3.5	4.9 (N=2)	4.1 (N=2)	3.2 (N=2)
	300 mT/m	4.3	3.5	2.8	3.7 (N=4)	3.1 (N=4)	2.4 (N=4)
3) Fibre dispersion $\kappa=16$	60 mT/m	7.7	6.4	5.0	7.7 (N=2)	6.3 (N=2)	4.9 (N=2)
	80 mT/m	6.8	5.7	4.4	6.7 (N=2)	5.4 (N=2)	4.2 (N=2)
	150 mT/m	5.2	4.4	3.4	4.9 (N=4)	4.1 (N=4)	3.2 (N=4)
	300 mT/m	4.1	3.4	2.7	3.7 (N=4)	3.0 (N=4)	2.4 (N=4)

Table 1: The table shows the smallest axon diameter a_0 below which one cannot distinguish from zero. The shaded values are the lowest possible a_0 across different N.

REFERENCES [1] Gore NMR BioMed 2010; [2] Drobnjak JMR 2010; [3] Drobnjak JMR 2011; [4] Li JMR 2014; [5] Siow JMR 2012; [6] Shemesh JMR 2013; [7] Assaf NeuroImage 2005; [8] Alexander MRM 2008; [9] Zhang NeuroImage 2012; [10] Ianus JMR 2013; [11] Drobnjak Microporous and Mesoporous Materials 2013.